European Journal of Neuroscience

European Journal of Neuroscience, Vol. 27, pp. 2907–2921, 2008 doi:10.1111/j.1460-9568.2008.06239.x

Targeted mutation of the calbindin D_{28K} gene disrupts circadian rhythmicity and entrainment

Lance J. Kriegsfeld,[1] Dan Feng Mei,[2] Lily Yan,[3] Paul Witkovsky,[5] Joseph LeSauter,[2] Toshiyuki Hamada[4] and Rae Silver[2,3,6]

[1]Department of Psychology and Helen Wills Neuroscience Institute, 3210 Tolman Hall, University of California, Berkeley, CA 94720, USA
[2]Department of Psychology, Barnard College, New York, NY, USA
[3]Department of Psychology, Columbia University, New York, NY, USA
[4]Age Dimension Research Center, National Institute of Advanced Industrial Science and Technology, Central 6, 1-1-1 Higashi, Tsukuba, Ibaraki 305-8562, Japan
[5]Department of Ophthalmology, New York University School of Medicine, New York, NY, USA
[6]Department of Pathology and Cell Biology, Columbia University Health Sciences Center, Columbia University, New York, NY, USA

Keywords: arrhythmic, clock gene, knockout, suprachiasmatic

Abstract

The suprachiasmatic nucleus (SCN) is the principal circadian pacemaker in mammals. A salient feature of the SCN is that cells of a particular phenotype are topographically organized; this organization defines functionally distinct subregions that interact to generate coherent rhythmicity. In Syrian hamsters (*Mesocricetus auratus*), a dense population of directly retinorecipient calbindin D_{28K} (CalB) neurons in the caudal SCN marks a subregion critical for circadian rhythmicity. In mouse SCN, a dense cluster of CalB neurons occurs during early postnatal development, but in the adult CalB neurons are dispersed through the SCN. In the adult retina CalB colocalizes with melanopsin-expressing ganglion cells. In the present study, we explored the role of CalB in modulating circadian function and photic entrainment by investigating mice with a targeted mutation of the CalB gene (CalB−/− mice). In constant darkness (DD), CalB−/− animals either become arrhythmic (40%) or exhibit low-amplitude locomotor rhythms with marked activity during subjective day (60%). Rhythmic clock gene expression is blunted in these latter animals. Importantly, CalB−/− mice exhibit anomalies in entrainment revealed following transfer from a light : dark cycle to DD. Paradoxically, responses to acute light pulses measured by behavioral phase shifts, SCN FOS protein and *Period1* mRNA expression are normal. Together, the developmental pattern of CalB expression in mouse SCN, the presence of CalB in photoresponsive ganglion cells and the abnormalities seen in CalB−/− mice suggest an important role for CalB in mouse circadian function.

Introduction

In mammals, circadian rhythms in physiology and behavior are generated by the suprachiasmatic nucleus (SCN) located in the anterior hypothalamus (Moore & Eichler, 1972; Stephan & Zucker, 1972). At the cellular level, rhythms are driven by an autonomous transcription–translation feedback loop (Okamura *et al.*, 2002; Panda *et al.*, 2002a; Schibler, 2005), although not all SCN cells express detectable oscillations (Hamada *et al.*, 2001; Jobst & Allen, 2002; Karatsoreos *et al.*, 2004a). Instead, the SCN is functionally compartmentalized, with light input and oscillatory time-keeping machinery being spatially segregated (Moore, 1996; Hamada *et al.*, 2001, 2003; Antle *et al.*, 2003; Karatsoreos *et al.*, 2004a).

In Syrian hamsters (*Mesocricetus auratus*), a retinorecipient ‘core’ SCN subregion marked by calbindin D_{28K} (CalB)-containing cells exhibits light-induced *Period* (*Per*) gene expression, whereas a separate ‘shell’ subregion expresses *Per* rhythmically (Bryant *et al.*, 2000; Hamada *et al.*, 2001). Although not detectably rhythmic in clock gene expression, the CalB subregion is critical for the maintenance of circadian function at the behavioral level (LeSauter & Silver, 1999; Kriegsfeld *et al.*, 2004). A similar organization occurs in the core region of the mouse SCN, where retinal afferents synapse directly onto gastrin-releasing peptide (GRP) cells that themselves do not have detectable rhythms in clock gene expression (Karatsoreos *et al.*, 2004a). In our model, core cells serve to reduce the phase dispersion among individual cellular oscillators in SCN shell (Antle *et al.*, 2003; Antle & Silver, 2005).

CalB-containing cells mark a functionally distinct subregion critical for hamster SCN function (LeSauter & Silver, 1999; Kriegsfeld *et al.*, 2004), and the calbindin protein influences the response to photic cues (Hamada *et al.*, 2003). Additionally, CalB is expressed in the retina in many species (Wassle *et al.*, 1998; Bennis *et al.*, 2005; Chiquet *et al.*, 2005), suggesting a possible role in transmission of photic information to the SCN. To investigate the specific role of CalB in circadian function and entrainment, we used mice with a targeted mutation of the CalB gene (CalB−/−). Our data reveal a critical role for CalB in mouse circadian function, and point to distinct mechanisms underlying discrete phase shifts and entrainment.

Correspondence: Dr L. Kriegsfeld, as above.
E-mail: kriegsfeld@berkeley.edu

Received 20 December 2007, revised 20 March 2008, accepted 1 April 2008

Materials and methods

Animals and housing

Homozygous calbindin D_{28K} null mutant (CalB−/−) experimental animals and wild-type (WT) control littermates were used in these studies. CalB−/− mice were generated in the laboratory of Dr Michael Meyer as described previously (Airaksinen *et al.*, 1997). After they were brought to our laboratory, mice were backcrossed for at least six generations with C57BL/6 WT animals. Animals were maintained in a colony room with a 12 : 12 h light : dark (LD) cycle at 23 ± 2°C, and were provided with food and water *ad libitum* throughout the duration of the studies. All experimental protocols conformed to the Institutional Animals Care and Use Committee guidelines of Columbia University.

General interpretation of findings

In this work we share a general caveat that applies to all studies of mutant animals derived from a cross between two strains of mice. Because we did not specifically select for recombination events on chromosome 4, the chromosome containing the CalB gene, there is a possibility that the flanking genomic region maintains SV129 alleles, potentially accounting for differences between CalB−/− mice and their WT siblings. However, the identified anomalies are not seen in SV129 crosses (Wee *et al.*, 2002), arguing against this possibility for the present findings.

Genotype determination

Genotypes were determined by polymerase chain reaction (PCR) using genomic DNA obtained from the tails of mice at 3 weeks old. PCR was performed to determine the genotypes using the primers Cs3 (common primer; sequence 5′-GCAAGTAACTAATGGCATCG-3′), C2 (WT primer; 5′-TGCAGCGGCTAGTTTGAGAGTG-3′) and Pa1 (mutant primer; 5′-TGACTAGGGGAGGAGTAGAAG-3′). The PCR reaction was run in a thermocycler using the following program: 95°C for 2 min (one cycle); 95°C for 45 s, 60°C for 45 s and 72°C for 2 min (35 cycles); 72°C for 10 min (one cycle), and soaking at 4°C. The reaction mixture was run on a 1.75% agarose gel stained with ethidium bromide. The WT band appears at 753 base pairs and the knockout (KO; mutant) band appears at 226 base pairs.

Evaluation of locomotor behavior

All animals (n = 10 WT; n = 20 CalB KO) were housed individually in cages equipped with running wheels (17 cm diameter) connected to a computer (Dataquest, Data Sciences, St Paul, MN, USA). Cumulative counts were recorded every 10 min. Animals were initially housed in a 12 : 12 h LD (light intensity = 800 lux) cycle for a period of at least 2 weeks. In order to test endogenous rhythm generation, animals were transferred to constant darkness (DD) and monitored in DD for at least 3 weeks.

Evaluation of entrainment in a skeleton photoperiod

Light suppresses locomotor behavior in nocturnal animals, independent of its effects on the circadian system, a phenomenon called masking. Accordingly, we used a ‘skeleton’ photoperiod (Mrosovsky, 1999) to further evaluate entrainment in CalB−/− mice. WT and CalB−/− mice (n = 8/genotype) were housed individually in cages equipped with running wheels connected to a computer. Animals were exposed to two 1-h light pulses (light intensity = 800 lux) separated by 11 h. Animals were monitored for at least 3 weeks following the onset of the photoperiod.

Evaluation of light-induced behavioral responses

All animals were housed individually in cages equipped with a running wheel (17 cm diameter) connected to a computer. During this phase of the experiment, all animals were housed in DD. WT and CalB−/− animals were exposed to a 30-min light pulse (800 lux) at one of the following circadian times (CT): CT4, CT16 or CT22 (CT; CT12 = onset of activity). Locomotor behavior was recorded for a minimum of 2 weeks following the light pulse. Phase shifts in behavior following the light pulse were calculated using ClockLab software (Actimetrics, Evanston, IL, USA).

Histochemical procedures

Perfusion

Mice were deeply anesthetized (200 mg/kg pentobarbital, i.p.) and perfused intracardially with 50 mL saline followed by 100 mL 4% paraformaldehyde in 0.1 M phosphate buffer (PB), pH 7.3. For animals killed during the dark portion of the LD cycle or in DD, anesthetic was administered under dim red light and the head covered with a light-proof hood before and during perfusion.

Tissue processing

All antibodies and tissue processing (excluding melanopsin) have been previously described (LeSauter *et al.*, 2003; Karatsoreos *et al.*, 2004b; Yan & Silver, 2004; Kriegsfeld *et al.*, 2006). Briefly, brains were postfixed for 18–24 h at 4°C and cryoprotected in 20% sucrose in 0.1 M PB overnight. For retinal processing, the eyes were enucleated and hemisected to remove cornea and lens; the eyecups were fixed for an additional 1 h and then washed three times for 20 min each in PB. Some eyecups were cryoprotected in 30% sucrose overnight and frozen sections, 14 μm thick, obtained. For retinal whole mounts, the retina was freed from the eyecup, processed for immunocytochemistry (see below) and mounted vitreal side up in VectaShield (Vector Laboratories, Burlingame, CA, USA).

Antibodies

Polyclonal antibodies raised against vasopressin and vasoactive intestinal peptide (VIP) (Incstar, Stillwater, MN, USA) were diluted at 1 : 10 000. The monoclonal CalB antibody (Sigma, St Louis, MO, USA) was used at 1 : 2000–20 000. c-FOS was raised in rabbit and applied at 1 : 10 000 (Santa Cruz Biotechnology, Santa Cruz, CA, USA). Rabbit anti-melanopsin (gift of Drs I. Provencio and M.D. Rollag, Uniformed Services University, USA) was used at 1 : 1000–1 : 2000. For clock protein staining, mPER1 (1 : 5000, gift of Drs S.M. Reppert and D.R. Weaver, University of Massachusetts, MA, USA) or mPER2 (1 : 5000, Alpha Diagnostics, San Antonio, TX, USA) antibodies were employed. Fluorescent secondary antibodies were goat anti-mouse Cy3 (1 : 200; Jackson Laboratories, West Grove, PA, USA) and goat anti-rabbit Cy2 (1 : 400, Molecular Probes).

Brain immunohistochemistry

Thirty-five-micrometer cryostat sections were processed free floating. Single-labeled brain sections were processed with a modified avidin-biotin-immunoperoxidase technique using diaminobenzidine (DAB; Sigma) as the chromogen. Double-labeled sections were incubated in donkey serum for 1 h, then in the two primaries made in different host species for 48 h, and then in the appropriate donkey secondary conjugated to the Cy2 and Cy3 fluorescent chromogens (1 : 200; Jackson ImmunoResearch) for 2 h. Sections were mounted and coverslipped with Permount (Fisher Scientific, Houston, TX, USA) for DAB, or Krystalon (EMD Chemicals, Gibbstown, NJ, USA) for Cy2 and Cy3. To test for specificity, primary antibodies were omitted in some runs (vasopressin, VIP, FOS, melanopsin, CalB, mPER1), preadsorbed with their antigenic peptides (melanopsin; 180 ng/mL) or applied to a KO model (CalB). To control for differences in staining for each round of immunohistochemistry, an equal number of animals from each condition were processed during each run.

Expression of CalB during development and adulthood

WT mice were killed at either postnatal day 10 (P10), P16 or in adulthood (> 60 days old; *n* = 5/group). Brains were labeled immunohistochemically using a mouse anti-CalB antibody.

Examination of melanopsin-immunoreactive retinal ganglion cells for CalB expression

Mice were killed at different Zeitgeber times (ZT; lights on = ZT0) or CT times as described above. Retinal sections or whole mounts were washed 3 × 10 min in phosphate-buffered saline (PBS), immersed for 1 h in a blocking solution (0.1% Na-azide, 0.1% Triton X-100, 1% bovine serum albumin in PBS), then incubated in the primary antibodies (rabbit melanopsin; mouse CalB; Panda *et al.*, 2002b) for 16–20 h at room temperature. Thereafter the tissue was washed for 6 × 10 min in PBS and incubated for 2 h in the fluorescent secondary antibodies. After a final series of washes, sections or whole mounts were covered in Vectashield. Control experiments included: omission of the primary antibodies; preadsorption of the primary antibody with the antigenic peptide (melanopsin); and testing for antibody immunoreactivity in a KO animal (CalB). Preadsorption was achieved by combining undiluted primary antibody with its antigenic peptide (180 ng/mL) for 12 h at 4°C, then applying the mixture as described above for the primary antibody alone.

Evaluation of rhythmic PER2 protein and vasopressin peptide expression

Rhythmic PER2 expression was evaluated under both a LD cycle and during free-running conditions in DD (*n* = 8/genotype/time point). Vasopressin expression was evaluated only during free-running conditions (*n* = 8/genotype/time point). In LD, brains were collected at ZT0, 4, 8, 12, 16 and 20 (lights on = ZT0). In DD, brains were collected at CT0, 4, 8, 12, 16, 20 (onset of activity = CT12). Brains were stained immunohistochemically and the data quantified as described below.

Evaluation of VIP cell numbers

VIP expression was investigated in WT and CalB−/− animals (*n* = 5/genotype) killed during the middle of the LD cycle (∼ZT6). Brains were stained immunohistochemically and VIP cells were counted in every fourth 40-μm section throughout the rostro-caudal extent of the SCN.

Evaluation of light-induced Period gene and FOS protein expression

For light-induced *mPer1* mRNA and FOS studies, mice (*n* = 5/genotype/condition) were maintained in DD for at least 2 weeks. All WT mice, and those CalB−/− mice demonstrating low-amplitude rhythms, were exposed to a 30-min light pulse (1000 lux) at one of the following circadian times: CT4, 16 or 22. Animals were killed 1 h following the start of the light pulse. Control animals for light-induced *mPer1* mRNA and FOS were also maintained in DD for at least 2 weeks, not exposed to light and killed at the same CT as experimental animals (*n* = 4/group). SCN core and shell were parsed based upon the pattern of vasopressin in alternate sections.

In situ *hybridization*

For *mPer1* mRNA *in situ* hybridization, alternate sections (30 μm) were processed free-floating. Brains were marked for identification and both genotypes were run in the same wells. To detect *mPer1*, *in situ* hybridization histochemistry was performed as described previously (Yan & Okamura, 2002). In brief, tissue sections were processed with proteinase K (1 μg/mL, 0.1 M Tris buffer, pH 8.0, 50 mM EDTA) for 10 min at 37°C and 0.25% acetic anhydride in 0.1 M triethanolamine for 10 min. Sections were incubated in hybridization buffer (60% formide, 10% dextran sulfate, 10 mM Tris-HCl, pH 8.0, 1 mM EDTA, pH 8.0, 0.6 M NaCl, 500 mg/mL 0.2% *N*-laurylsarcosine, 200 mg/mL tRNA, 1 × Denhardt's solution, 0.25% SDS and 10 mM dithiothreitol) containing digoxigenin-labeled *mPer1* antisense cRNA probe for 16 h at 60°C. After a high-stringency posthybridization wash, sections were treated with RNaseA, then further processed for immunodetection with a nucleic acid detection kit (Boehringer Mannheim, Indianapolis, IN, USA). Thereafter, sections were incubated in a blocking reagent diluted 1 : 100 in buffer 1 (in mM: Tris-HCl buffer, 100; NaCl, 150; pH 7.5) for 1 h at room temperature, then incubated at 4°C in an alkaline phosphatase-conjugated digoxigenin antibody diluted 1 : 5000 in buffer 1 for 3 days. On the following day, sections were washed in buffer 1 twice (2 × 5 min each) and incubated in buffer 3 (1 × 5 min, 100 mM Tris-HCl buffer, pH 9.5, containing 100 mM NaCl and 50 mM $MgCl_2$). Sections were then incubated in a solution containing nitroblue tetrazolium salt (0.34 mg/mL) and 5-bromo-4-chloro-3-indolyl phosphate toluidinium salt (0.18 mg/mL; Roche, Indianapolis, IN, USA) for 8 h. The colorimetric reaction was halted by immersing the sections in buffer 4 (10 mM Tris-HCl containing 1 mM EDTA, pH 8.0). Sections were mounted on slides and coverslips were applied with Permount (Fisher Scientific). Alternate sections were matched with their adjacent sections from the immunocytochemistry runs for analysis.

Microscopy and quantification

SCN borders and subregions were delineated based on vasopressin staining in adjacent sections. For quantification of optical density (OD), images of serial sections through the SCN were captured using a CCD video camera (Sony XC77) attached to a light microscope (BH-2; Olympus Optical, Tokyo, Japan). mRNA expression was quantified using the NIH Image program (version 1.61). Relative OD, assessing the mean gray value per pixel, was used to quantify the intensity of the signal in the SCN compared with the adjacent hypothalamic area. The ratio of the SCN density to the background was the value for each section. The average ratio of the sections from each brain was used as the value for one animal. Fluorescently stained sections were excited using filters for CY2 and CY3. Images were processed using Photoshop 7 (Adobe Systems, Mountain View, CA, USA).

Analyses and statistics

The power of all rhythms was assessed using a Fourier analysis (Dataquest or Clocklab programs). An animal was considered rhythmic when the highest peak occurred at ∼1 cycle/day, with an absolute power of at least 0.005 mV/Hz. For assessment of rhythmic staining across the day, 2 (genotype) × 6 (time) analyses of variance (ANOVA) were used. To assess light-induced responses, 2 (genotype) × 3 (time point) ANOVA were used. Results were considered significant when $P < 0.05$.

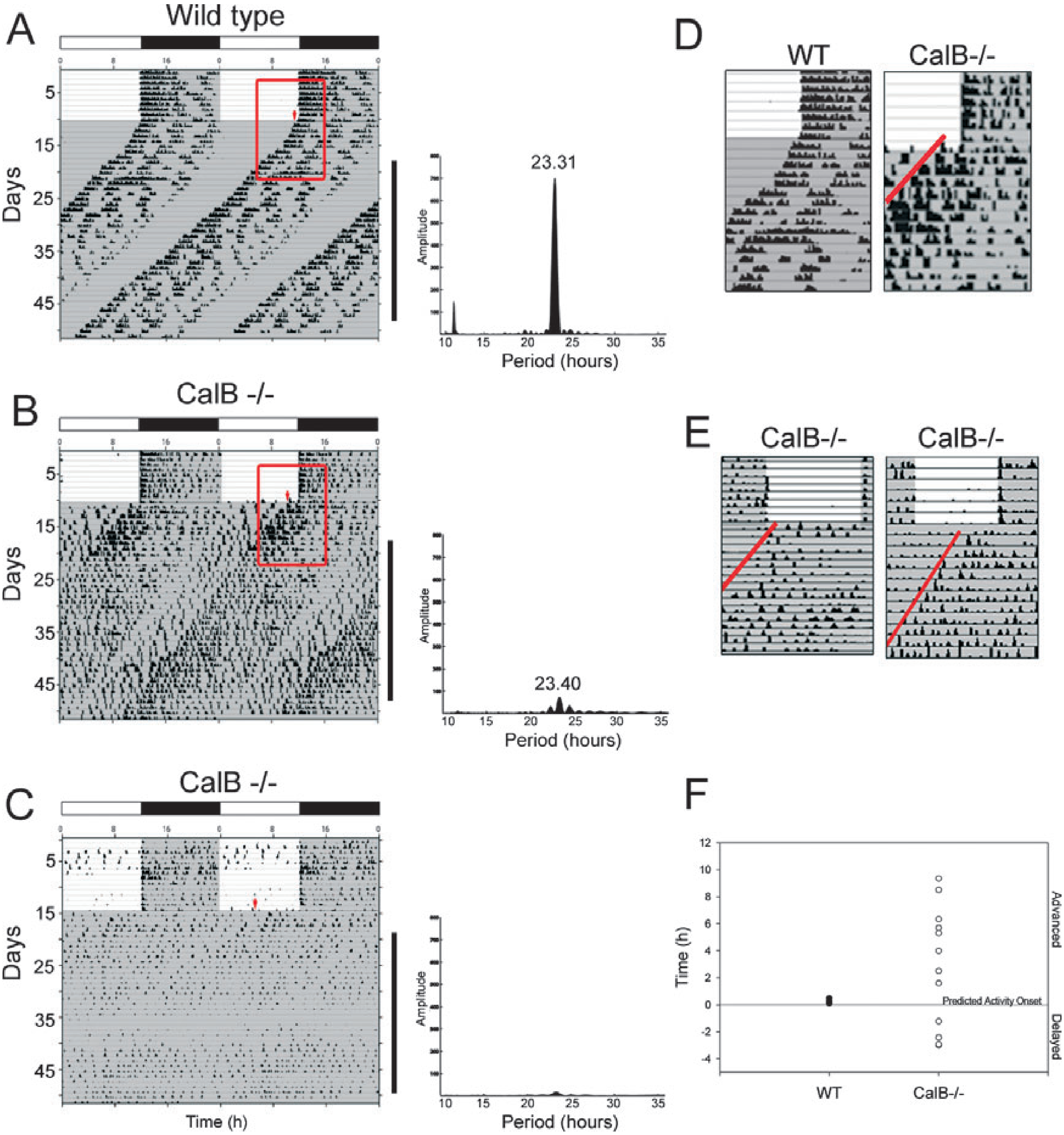

FIG. 1. Calbindin D$_{28K}$ (CalB) −/− mice exhibit pronounced abnormalities in circadian rhythms and entrainment. Activity records from animals initially held in a 12 : 12 LD cycle then transferred to DD. Wild-type (WT) animals demonstrate entrainment in LD as indicated by the ability to predict activity onset when placed into DD (A). Approximately 60% of CalB−/− mice exhibit low-amplitude rhythms when transferred to DD. In these animals, although the majority of activity was confined to the dark period in LD, activity onset in DD was variable relative to the phase of LD behavior (B). Approximately 40% of CalB−/− mice become arrhythmic soon after exposure to DD (C). The red arrow points to onset of activity after transfer to DD. The red boxes in (A) and (B) outline areas enlarged in (D) that show activity onset in DD relative to the previous LD cycle. (E) Further examples of the random nature of activity onset following transition from LD to DD in CalB−/− mice. The onset of activity after transfer to DD, relative to the previous LD cycle, is shown quantified in (F). Shaded regions indicate periods of darkness mirrored in LD bars above the actograms.

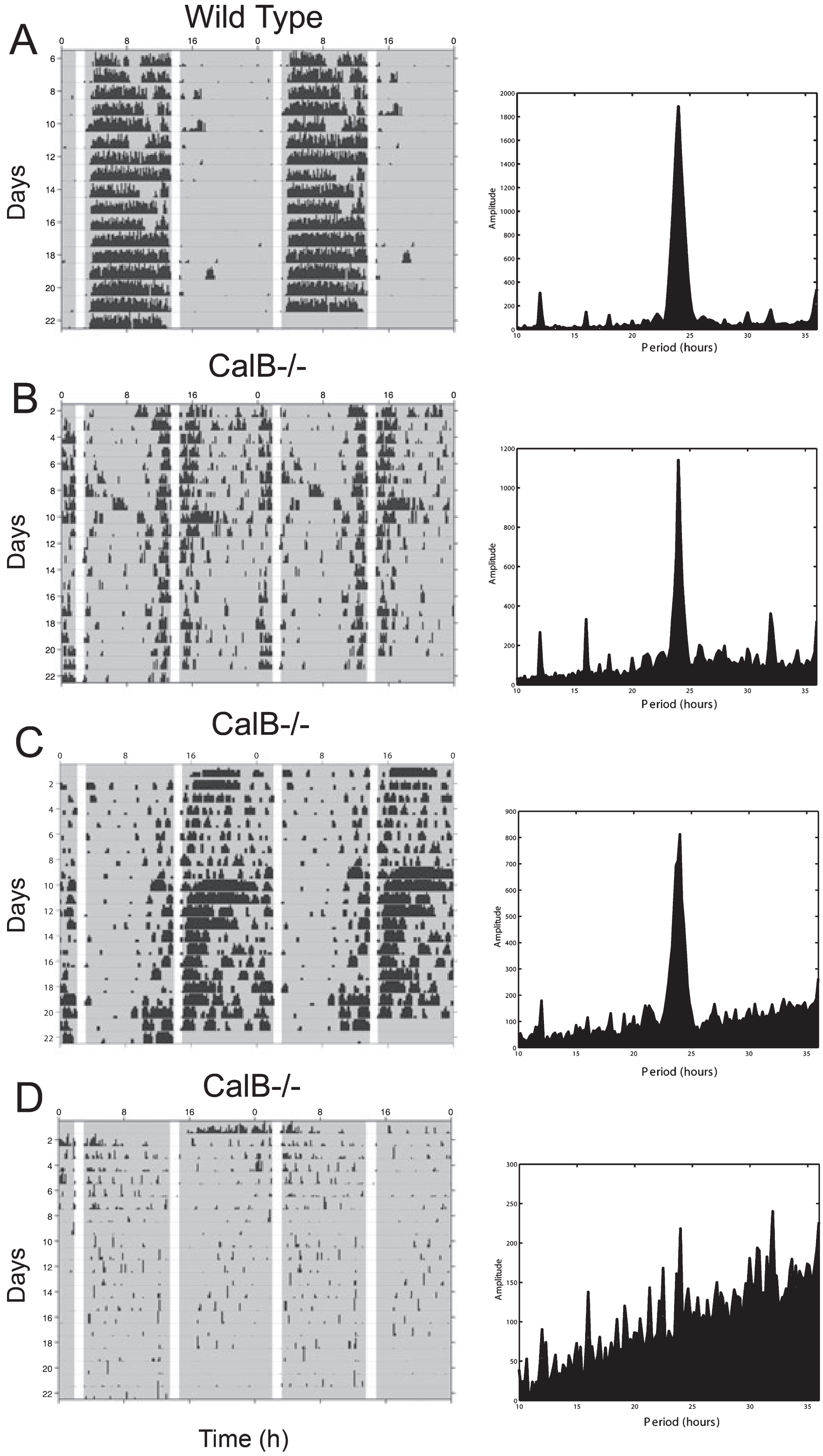

FIG. 2. Calbindin D_{28K} (CalB)−/− mice exhibit abnormal entrainment to a skeleton photoperiod. Representative activity records from one WT (A) and three CalB−/− animals (B–D) held in a skeleton photoperiod. WT mice synchronize their behavior to the two 1-h light pulses as if they were maintained in a complete LD cycle. Rhythmic CalB−/− mice exhibited more activity throughout both dark periods compared with WT mice. Animals in (B) and (D) show signs of entrainment as manifested by the production of a 24-h rhythm and entrainment with an abnormal phase angle. Arrhythmic CalB−/− mice exhibit equal amounts of activity throughout both dark periods, with masking during brief periods of light. Shaded regions of the activity records indicate periods of darkness.

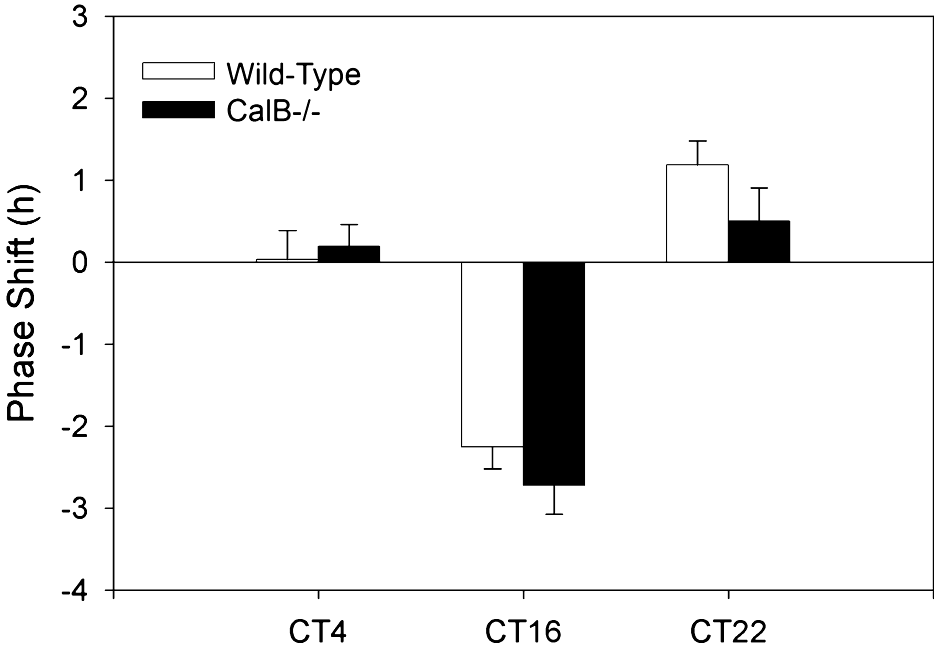

FIG. 3. Phase shifting is unaffected in calbindin D_{28K} (CalB) mutants. CalB−/− mice phase shift normally in response to light pulses during the subjective day [circadian time (CT)4] and night (CT16, CT22). Both WT and CalB−/− mice do not phase shift at CT4, and exhibit characteristic phase delays at CT16 and phase advances at CT22.

Results

CalB−/− mice exhibit abnormalities in circadian rhythms and entrainment

When housed in LD, both WT and CalB−/− animals exhibited a 24 h rhythm ($P < 0.05$), with virtually all activity confined to the dark period. When placed into DD, WT mice began activity at a time point predicted by their behavior in the previous LD cycle, indicating prior entrainment (Fig. 1A; $P < 0.05$). In contrast, when placed into DD, CalB−/− animals showed one of two phenotypes, either rhythmicity with low amplitude and substantial activity during subjective day (12 of 20 animals) or arrhythmicity (8 of 20 animals; $P < 0.05$ relative to WT and rhythmic CalB−/− mice; Fig. 1B and C). Rhythmic CalB−/− animals began activity in DD at a random time point relative to the previous LD cycle (Fig. 1B, D and E; $P < 0.05$ relative to WT mice). This finding further suggests that CalB−/− mice were not synchronized to the previous LD cycle, but were instead masked during light exposure. Because it is not possible to determine whether animals that are not entrained were phase advanced or delayed relative to the previous LD cycle, the designation of 'advanced' vs. 'delayed' is arbitrary in Fig. 1F. However, the timing of activity onset can readily be observed. When placed into DD, the period of WT animals (23.45 ± 0.11 h) did not differ from that of the CalB−/− mice rhythms (23.38 ± 0.09 h; $P > 0.05$), measured in the rhythmic animals. The average number of wheel revolutions/10-min bin was reduced in CalB−/− mice compared with WT animals (1.55 ± 0.39 vs. 18.77 ± 1.73; $P < 0.05$). The duration of the activity bout in CalB−/− mice maintaining rhythmicity was not different from that of WT animals (14.98 ± 1.49 h vs. 14.10 ± 0.78 h; $P > 0.05$).

CalB−/− mice exhibit abnormal entrainment to a skeleton photoperiod

In order to further evaluate the abnormal entrainment of CalB−/− mice, WT and CalB−/− mice were investigated under a skeleton photoperiod. Under this experimental paradigm, two 'pulses' of light are interpreted as dawn and dusk, and WT rodents readily entrain as if exposed to a complete LD cycle. If animals are incapable of entraining, the pulses of light will mask activity and animals will free-run during the dark period. Under this skeleton photoperiod, all WT mice entrained to the two light pulses. They showed a clear 24-h period ($P < 0.05$) of wheel-running, with virtually all activity occurring during one of the dark bouts (Fig. 2A). In contrast, CalB−/− animals ran during both dark periods and were inactive during the 1-h light pulses (Fig. 2B–D). Arrhythmic CalB−/− animals ($n = 2$) lacking circadian activity rhythms ran equally during both dark periods. Importantly, rhythmic CalB−/− mice ($n = 6$) ran with a significant 24-h period ($P < 0.05$), with activity masked during the light pulses (Fig. 2C and D), suggesting an effect of light on circadian period, although entrainment was abnormal. Because animals were housed in DD prior to the skeleton photoperiod, the initial light pulses were differentially interpreted as dawn or dusk by each animal, resulting in some mice being active 180° out of phase with others.

Phase shifting is unaffected in CalB mutants

For all light pulse experiments, only those animals exhibiting low-amplitude rhythms were evaluated, as it is not possible to investigate the effects of discrete light pulses in arrhythmic animals, due to lack of a phase reference point. Because CalB−/− mice exhibited deficits in entrainment to an LD cycle, we investigated their phase-shifting behavior in response to acute light pulses. At all time points investigated (CT4, CT16, CT22), CalB−/− mice exhibited appropriate behavioral phase shifts of the same direction and magnitude seen in WT controls ($P > 0.05$ for each time point; Fig. 3).

Developmental changes in CalB expression in mouse SCN

CalB protein expression was greatest in the SCN at P10, with pronounced expression in the caudal SCN core. By P16, CalB

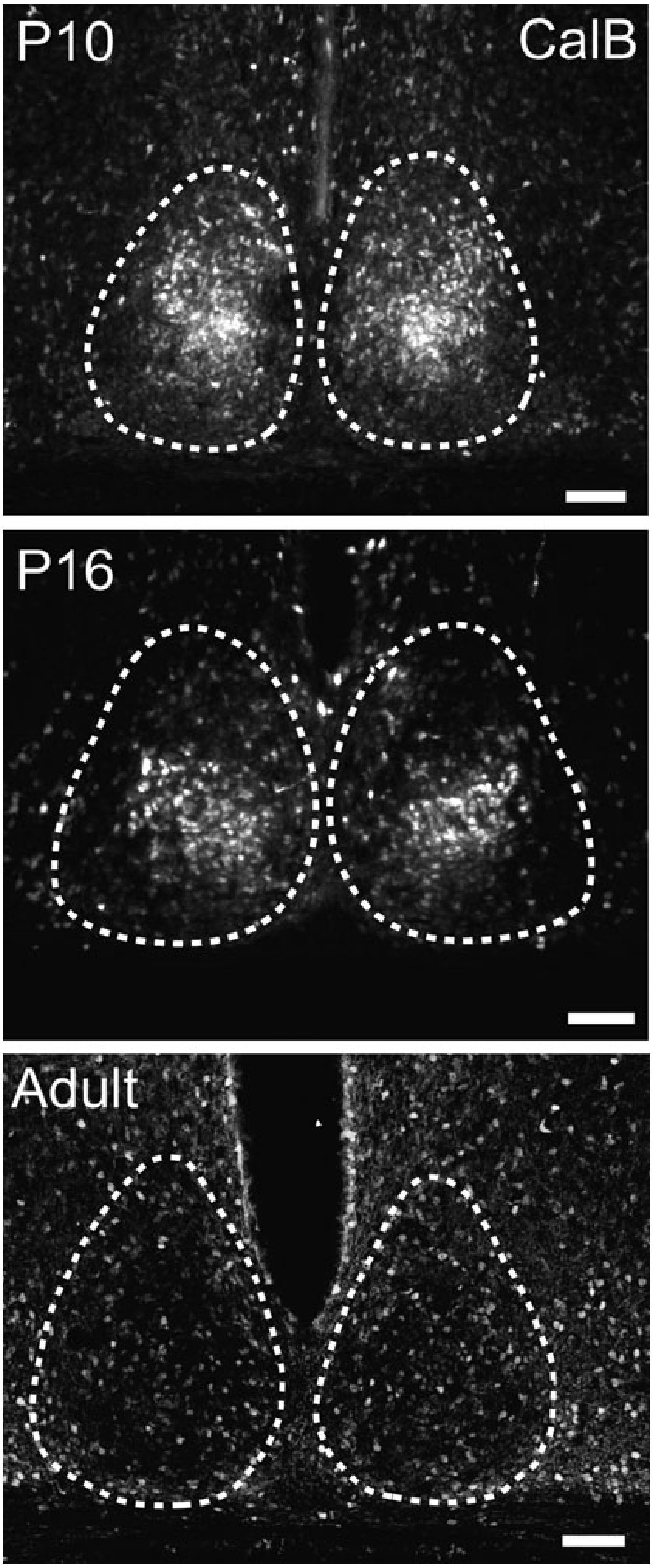

FIG. 4. Developmental changes in calbindin D_{28K} (CalB) expression in mouse SCN. Calbindin protein is expressed in SCN core early during postnatal development, with scattered expression in the adult mouse SCN. Photomicrographs depict CalB protein expression in the caudal SCN of WT mice at either postnatal day (P)10 (top), P16 (middle) or in adulthood (bottom). Dashed lines outline the SCN. Scale bar: 100 μm.

expression had diminished, but was still detectable and was concentrated in the same core subregion as that observed at P10. In contrast, adult animals exhibited scattered expression of CalB in SCN with no concentration of these cells at any rostro-caudal aspect (Fig. 4).

Melanopsin-immunoreactive retinal ganglion cells co-express CalB

Melanopsin-immunoreactive ganglion cell bodies are found primarily in the ganglion cell layer, with an additional population located at the border of inner nuclear and inner plexiform layers (Fig. 5). Multiple dendrites arising from these perikarya arborize throughout the inner plexiform layer, terminating in its most distal portion, near the border with the inner nuclear layer (Fig. 5E). On the basis of size, location and arborization patterns, these are the same melanopsin ganglion cells described earlier in mammalian retinas (Provencio *et al.*, 2000; Hattar *et al.*, 2002). In our material, the identity of these neurons as ganglion cells was confirmed by the observation that the labeled cells emitted axons. We examined this cell population for colocalization with CalB. As illustrated in Fig. 5A, the subset of ganglion cells expressing melanopsin is variable with regard to size and shape, and also in the intensity of melanopsin immunoreactivity. The most commonly observed melanopsin-immunoreactive ganglion cell was round to oval in shape, and 9–12 μm in diameter or long axis (see examples in Fig. 5A, D–F). Although melanopsin immunoreactivity was found throughout the perikaryon, it invariably was brightest just adjacent to the plasma membrane, as noted in previous reports (Hattar *et al.*, 2002).

Figure 5 illustrates colocalization of CalB and melanopsin. The most prominent CalB signal was in the cell nucleus and sometimes confined to that location, though in some instances CalB was in both cell nucleus and perikaryal cytoplasm (Fig. 5C). An examination of 953 melanopsin ganglion cells in six retinas revealed that the percentages of melanopsin ganglion cells expressing CalB ranged from 31 to 54%. Figure 5E and F illustrates that the CalB signal was absent in CalB−/− mice. Figure 5G–I illustrates controls for the specificity of the melanopsin. Melanopsin was present in control tissue (Fig. 5G) but absent when the primary antibody was preadsorbed with its antigenic peptide (Fig. 5H). Melanopsin also was absent when the primary antibody was omitted (Fig. 5I).

Deletion of CalB affects PER2 protein and vasopressin peptide expression

In order to determine if low-amplitude rhythms are associated with damped expression of clock or clock-controlled genes, the rhythmic patterns of PER2 protein and vasopressin expression were evaluated (Figs 6 and 7). In an LD cycle, PER2 expression began to rise later in CalB−/− mice relative to WT animals ($P < 0.05$ in each case). In DD conditions, PER2 expression was damped in CalB−/− mice ($P < 0.05$) and vasopressin expression was reduced at all time points ($P < 0.05$ in each case), excluding CT16.

Evaluation of VIP cell numbers

To test whether the reduction in vasopressin expression in CalB−/− mice was due to a non-specific reduction of SCN peptides in CalB−/− mouse SCN, we examined SCN expression of VIP. In contrast to vasopressin, we did not observe any differences in VIP expression between WT and CalB−/− mice (Fig. 8).

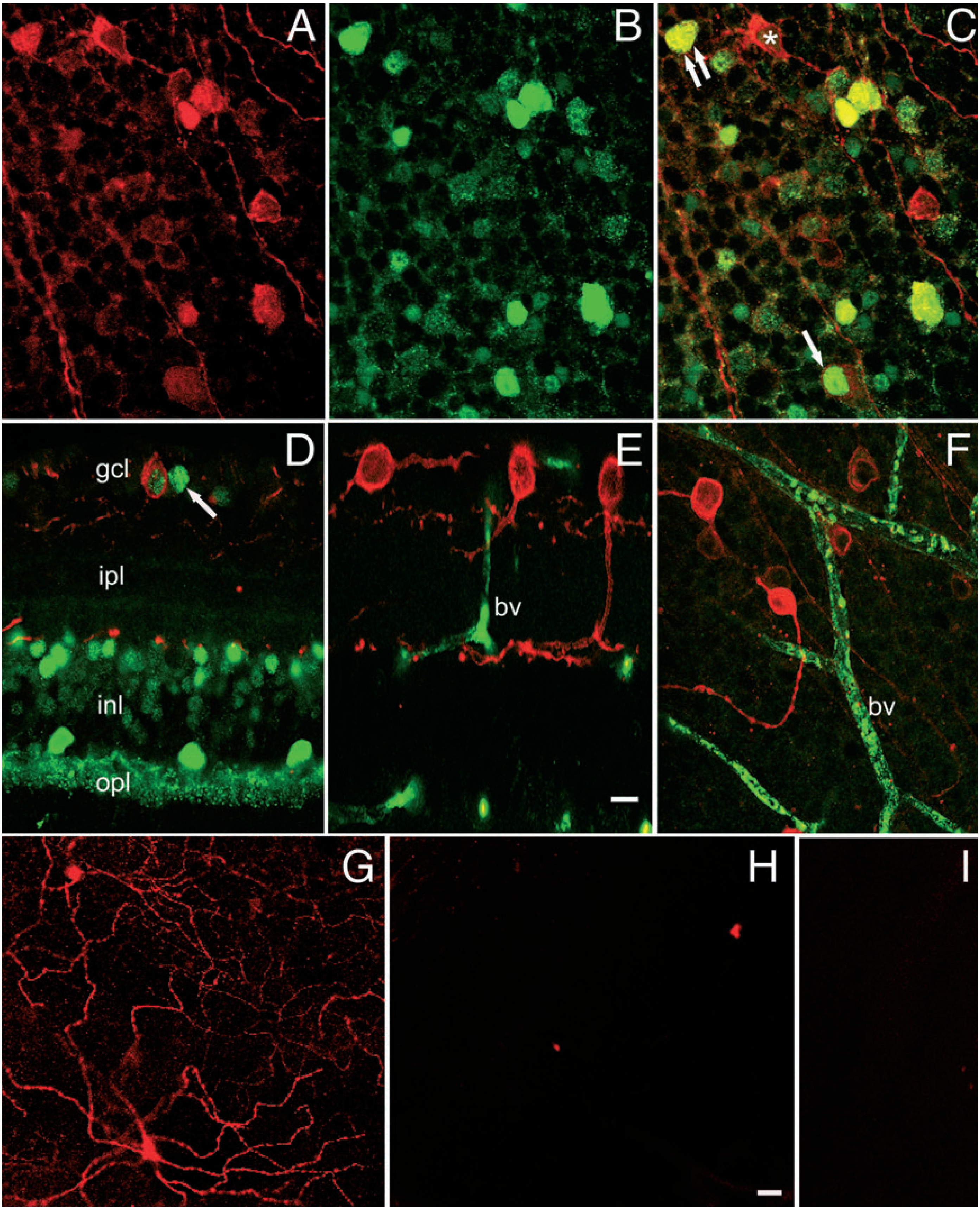
A
B
C
*
D
gcl
ipl
inl
opl
E
bv
F
bv
G
H
I

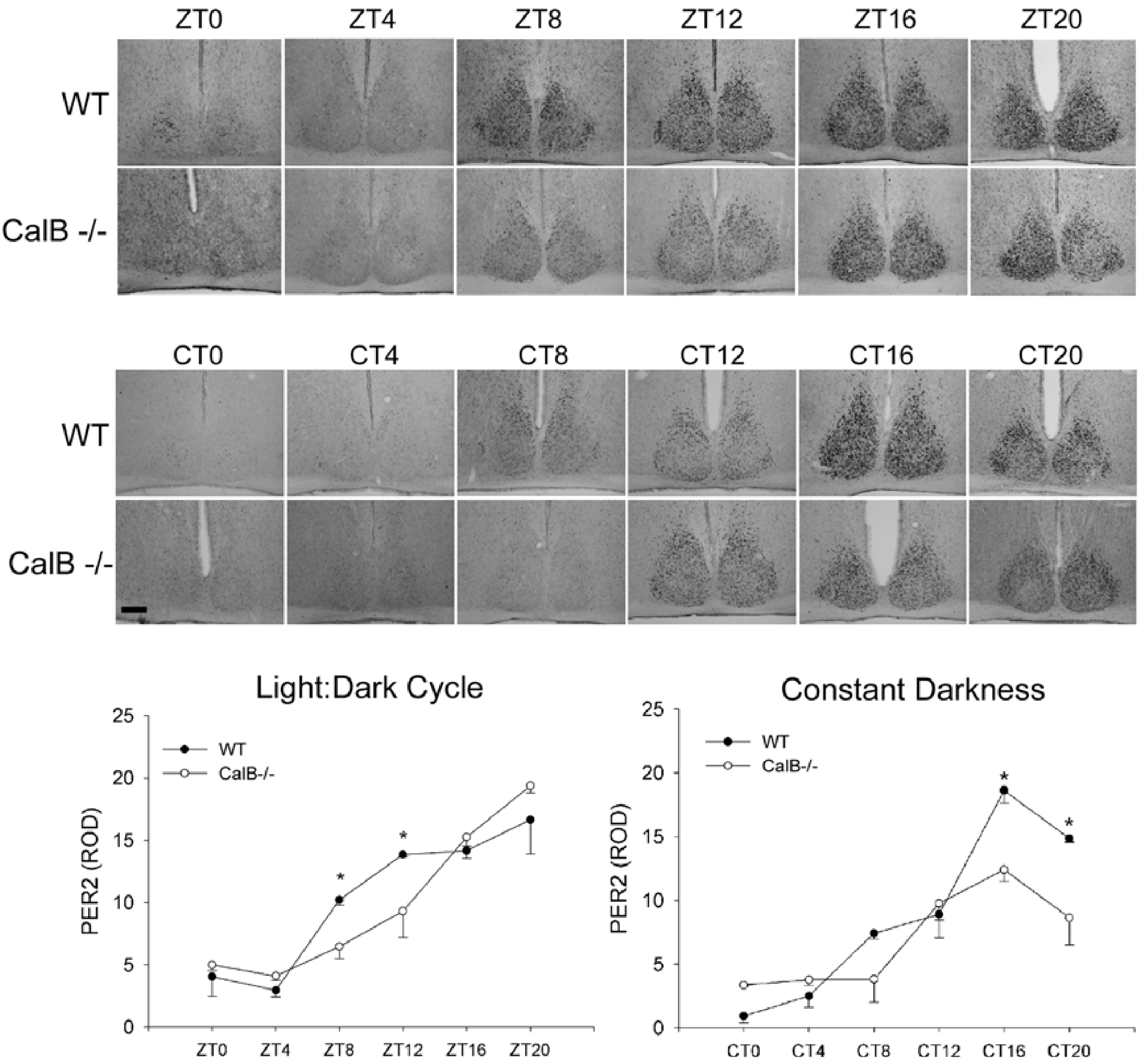

FIG. 6. Rhythmic PER2 expression. Pattern of PER2 protein expression across the day in animals held in a 12 : 12 h LD cycle (Zeitgeber time; ZT) or in DD (circadian time; CT). Photomicrographs depict PER2 expression in the SCN that is quantified in the graphs. Both in LD and DD, pronounced disruptions in the amplitude of clock gene expression are noted. *Significantly greater than calbindin D_{28K} (CalB)−/− animals at the same time point. Scale bar: 100 µm. ROD, relative optical density; WT, wild-type.

FIG. 5. Colocalization of calbindin and melanopsin. (A) Melanopsin (red); (B) calbindin (green); (C) merged image from retinal whole mount focused on ganglion cell layer. Single arrow: melanopsin ganglion cell in which calbindin is confined to the nucleus. Double arrow: melanopsin ganglion cell in which calbindin is found in both nucleus and perikaryal cytoplasm. Asterisk: melanopsin ganglion cell lacking calbindin. (D) Vertical section of WT retina showing layers: gcl, ganglion cell layer; inl, inner nuclear layer; ipl, inner plexiform layer; opl, outer plexiform layer. Multiple retinal cell types show calbindin immunoreactivity. A melanopsin ganglion cell with a calbindin signal is seen in gcl. The arrow indicates calbindin-immunoreactive ganglion cell lacking melanopsin immunoreactivity. (E) Vertical section of calbindin KO retina. No calbindin immunoreactivity is seen, but non-specific label is noted in blood vessels (bv). (F) Whole mount preparation of CalB−/− retina. Note both bright and dim melanopsin-immunoreactive ganglion cells. The marker bar (10 µm) in (E) applies to layers (A–F). (G–I) Anti-melanopsin immunoreactivity is present in control retina (G), but is lacking in preadsorption control (H) and when the primary anti-melanopsin antibody was omitted (I). The 20-µm marker bar in (H) applies to (G–I).

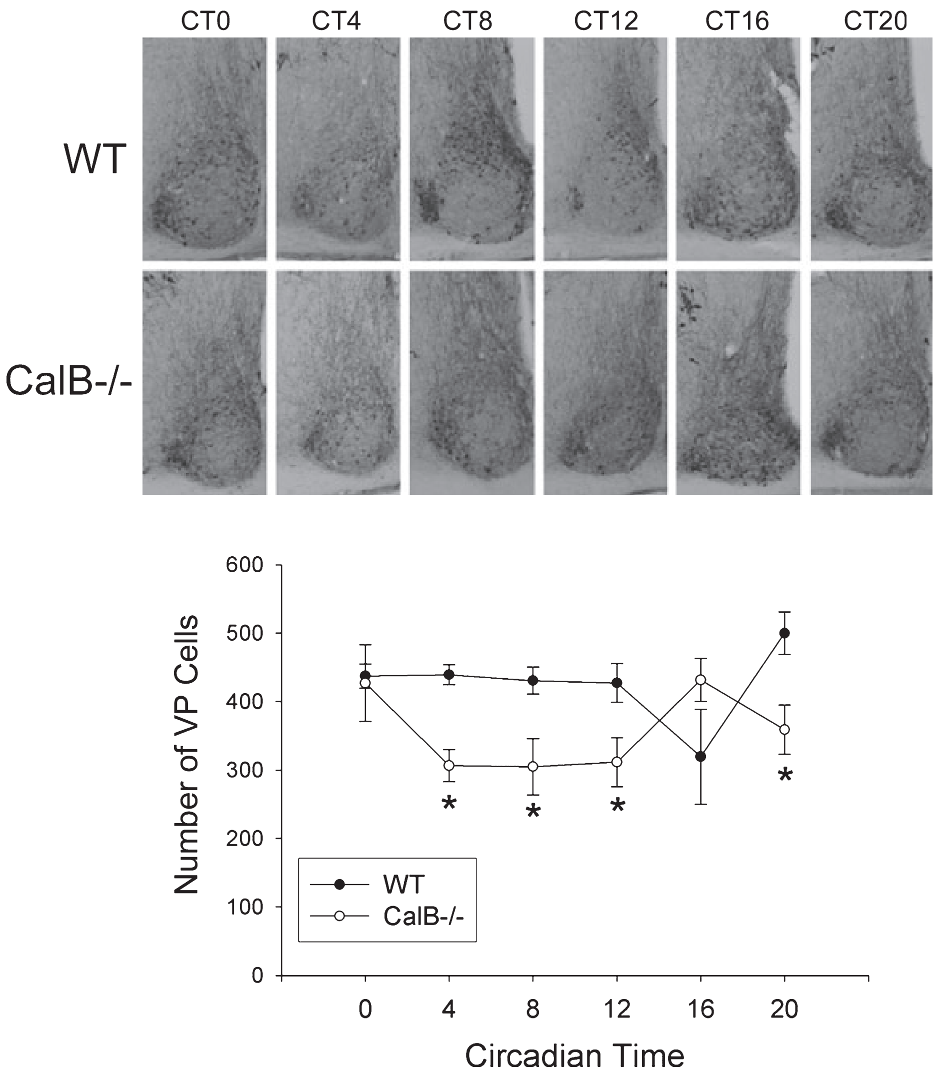

FIG. 7. Vasopressin expression is affected by deletion of calbindin D_{28K} (CalB). Photomicrographs depicting the rhythm of vasopressin peptide (VP) expression in wild-type (WT) and CalB−/− animals held in DD. Images are shown for the middle region of the SCN. Quantified cell counts indicate a blunted vasopressin expression in CalB−/− mice relative to WT controls (bottom). *Significantly less than WT animals at the same time point. Scale bar: 100 μm. CT, circadian time.

Effect of CalB deletion on light-induced Period gene and FOS protein expression

To evaluate whether light-induced SCN gene activation was altered in CalB−/− mice, we exposed mice to a light pulse presented at different times of subjective day and night. The results indicate that light-induced *mPer1* occurs primarily during the subjective night, with no differences seen between WT and CalB−/− mice at any time point investigated in either the SCN core or shell ($P > 0.05$ in all cases; Fig. 9). During subjective day, increased *mPer1* expression is observed in WT SCN core ($P < 0.05$), with a similar increase in CalB−/− mice that did not reach statistical significance ($P > 0.05$). Similar results were obtained with light-induced FOS expression (Fig. 10), although an ANOVA indicated that, overall, light-induced FOS expression was reduced in the SCN of CalB−/− mice compared with WT animals ($P < 0.05$). Comparisons of FOS expression at individual time points revealed a significant reduction in shell FOS expression in CalB−/− animals at CT16 and CT22 ($P < 0.05$ in each case).

Discussion

The present findings indicate a fundamental role for CalB in circadian organization. The results show that a targeted deletion of CalB leads to striking abnormalities in circadian rhythms of locomotor activity, photic entrainment and gene expression, with attenuated rhythms of PER2 expression. CalB−/− mice either become arrhythmic (40%) or exhibit exceptionally low-amplitude circadian activity (60%) when housed in constant conditions. Additionally, CalB−/− mice exhibit abnormal entrainment to an LD cycle and a skeleton photoperiod, whereas the phase-shifting response to discrete light pulses is unaffected in these animals. Together with observations indicating marked SCN expression of CalB during development, along with CalB co-expression in adult melanopsin-expressing retinal ganglion cells, the present findings suggest a role for this protein in master clock organization and photic transduction.

The reduction in amplitude of circadian locomotor rhythmicity seen in those CalB−/− mice that maintained rhythmicity could be the result of a compromised circadian clockwork mechanism, its output, or

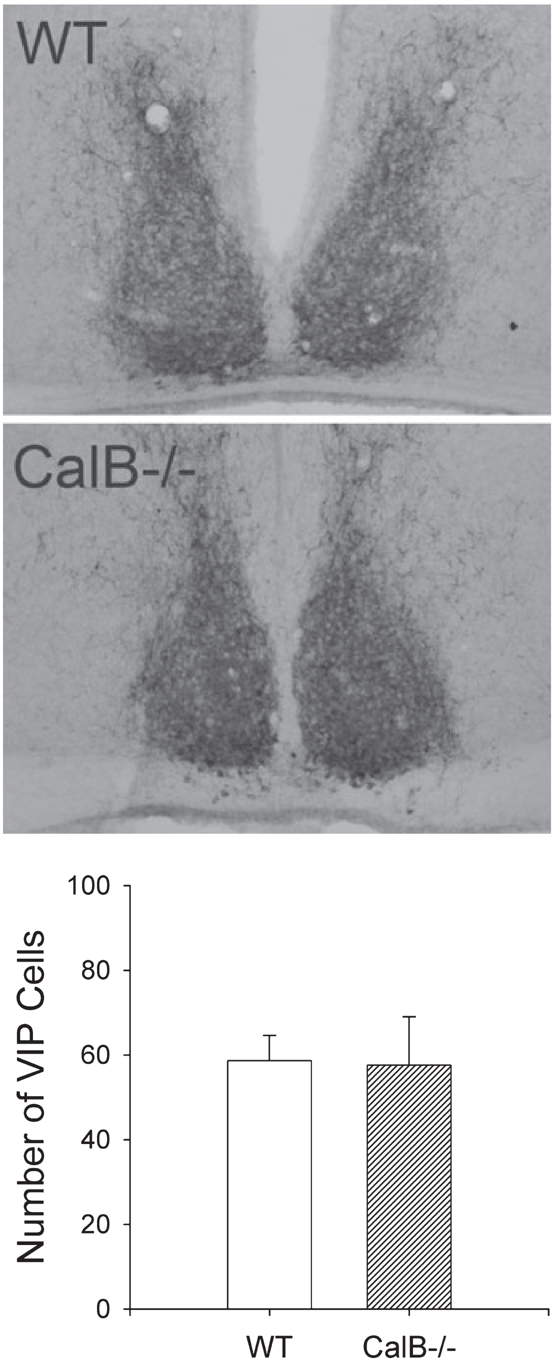

FIG. 8. VIP expression in the SCN of wild-type (WT) and calbindin D_{28K} (CalB)−/− mice. Representative photomicrographs of VIP-immunoreactive staining in the SCN of WT (top) and CalB−/− (bottom) mice. Unilateral counts of VIP-immunoreactive-labeled cells did not differ between genotypes (bottom).

alterations in downstream target systems. Reductions in PER2 amplitude, a key component of the core circadian clock (Okamura *et al.*, 2002; Panda *et al.*, 2002a; Schibler, 2005), observed in CalB−/− mice (Fig. 6) are consistent with compromised circadian clock function at the cellular or network levels. Moreover, vasopressin, a protein product of a rhythmically expressed clock-controlled gene (Jin *et al.*, 1999; Silver *et al.*, 1999), is reduced in the SCN of CalB−/− mice. The pattern of vasopressin expression seen in CalB−/− mice is in agreement with previous work (Van der Veen *et al.*, 2005). However, we failed to detect a similar rhythm in WT animals. As a result, one should be cautious in attributing deficits in clock function to alterations in vasopressin expression in the SCN of CalB−/− animals. CalB−/− mice are reported to exhibit mild ataxia, measured by slipping and falls in a runway test, that might contribute to their reduced locomotor amplitude. In their normal cage environment, however, these animals are indistinguishable from WT cage mates. In a horizontal rod balance test, CalB−/− animals exhibit minor deficits that disappear with additional training (Airaksinen *et al.*, 1997). It is nevertheless possible that the reductions in amount of wheel-running are the result of motor coordination deficits.

Despite the observation that entrainment appears normal when CalB−/− mice are housed in an LD cycle, three aspects of the results indicate abnormal entrainment in these animals. First, following transfer from LD to DD, CalB−/− mice began running at a variable phase relative to the previous LD cycle. In contrast, WT mice begin activity in DD around the time of prior dark onset (Fig. 1). Second, in contrast to their WT littermates, the nightly onset of activity in CalB−/− mice followed, rather than anticipated, darkness (Fig. 1B), suggesting that masking, and not entrainment, was occurring. Masking is independent of the action of light on the SCN (Mrosovsky, 1999) and is thought to be a consequence of aversion to light resulting in suppression of daytime activities. Third, whereas WT mice readily entrained to skeleton photoperiods, CalB−/− mice exhibited abnormal entrainment under these conditions (Fig. 2). WT mice interpret two appropriately spaced light ‘pulses’ as a complete LD cycle, whereas animals that do not entrain to this skeleton photoperiod typically free-run, with activity masked during brief periods of light (Mrosovsky, 1999). CalB−/− mice exhibit two phenotypes under these conditions. Arrhythmic CalB−/− mice exhibit disorganized circadian behavior, whereas animals expressing detectable rhythms under these conditions exhibit a 24-h period, although their behavior is not synchronized to the skeleton light pulses. Had CalB−/− mice been unaffected by the light pulses during the skeleton photoperiod they would be expected to free-run with a period less than 24 h, as seen in DD conditions. Finally, rodents can entrain to light intensities of ~1 lux (Foster *et al.*, 1991; Nelson & Takahashi, 1991a,b; Berson *et al.*, 2002). In the present study, lights of 800 lux, well above threshold for either entrainment in LD or in skeleton photoperiods, failed to entrain CalB−/− mice. Together, these findings indicate that a functional component of the entrainment mechanism is disrupted in animals lacking CalB.

Whereas CalB−/− mice exhibit abnormal entrainment relative to WT animals, the response to discrete light pulses appears to be intact. CalB−/− mice do not differ from WT animals in behavioral phase shifts, with light induction of *mPer1* and FOS protein being minimally attenuated. Although behavioral phase shifts were not observed for light pulses presented at CT4, small increases in *mPer1* and FOS were uncovered. The pattern and amplitude of expression were far less than that seen following light pulses presented during subjective night, with no differences observed between genotypes.

Disruptions in circadian rhythm generation in CalB−/− mice point to anomalous function in the SCN in these animals. A core subregion of hamster SCN delineated by a cluster of CalB-expressing cells is essential for circadian rhythmicity *in vivo* (LeSauter & Silver, 1999; Kriegsfeld *et al.*, 2004). A functionally similar topographical organization is seen in mouse SCN (Karatsoreos *et al.*, 2004a). The fact that CalB−/− mice exhibit pronounced disruptions in circadian function, along with the observation that CalB is expressed in the SCN core in the early postnatal period, suggest that CalB is important for the functional development of SCN circuitry (Antle *et al.*, 2003, 2007).

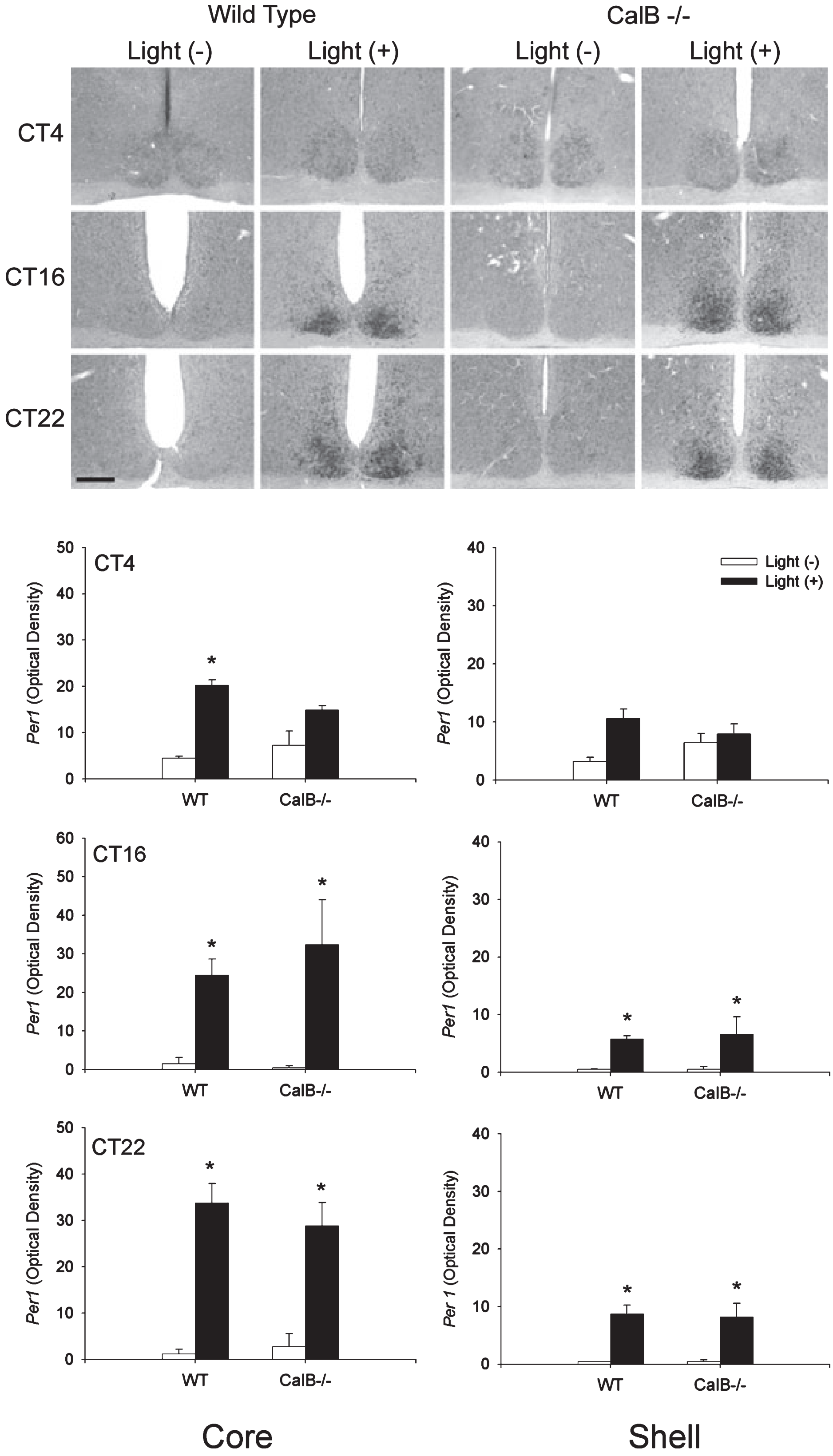

FIG. 9. Light-induced mPer1 expression is not affected in calbindin D$_{28K}$ (CalB)−/− mice. Medium-power photomicrographs depict the pattern of *mPer1* expression in animals exposed to a light pulse (light +) at circadian time (CT)4, CT16 or CT22, or control animals killed at the same time that were not exposed to a light pulse (light –) (top). Graphs depict quantified *mPer1* expression in the SCN core (left) and shell (right) of wild-type (WT) and CalB−/− mice. Animals did not differ on any of the parameters investigated. Scale bar: 100 μm. *Significantly greater than light (−) animals of the same genotype ($P < 0.05$).

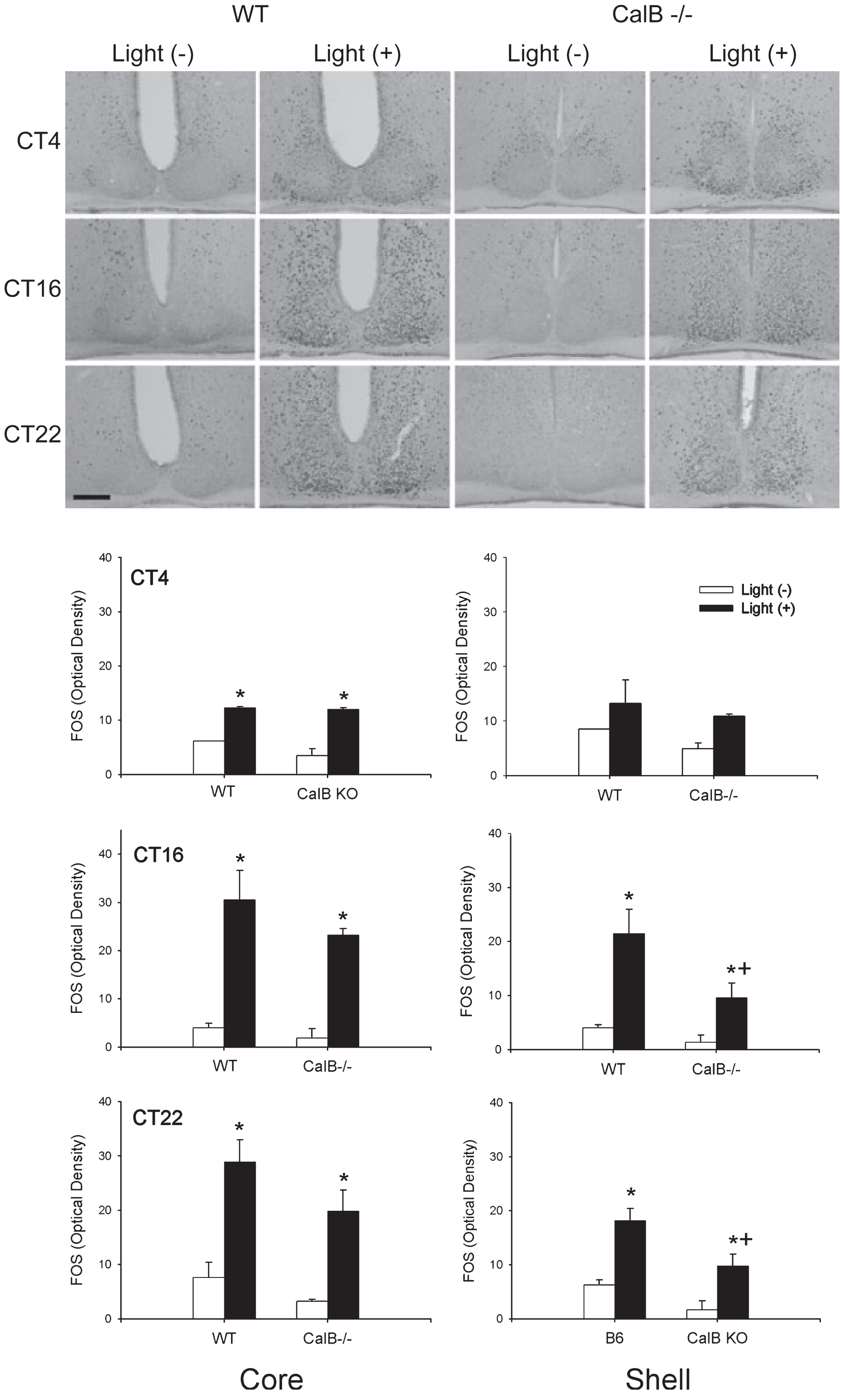

FIG. 10. Light-induced FOS expression is minimally reduced in calbindin D_{28K} (CalB)−/− mice. Medium-power photomicrographs depict the pattern of FOS expression in animals exposed to a light pulse (light +) at circadian time (CT)4, 16 or 22, or control animals killed at the same time that were not exposed to a light pulse (light –) (top). Graphs depict quantified FOS expression in the SCN core (left) and shell (right) of wild-type (WT) and CalB−/− mice. Scale bar: 100 μm. *Significantly greater than light (−) controls from the same genotype; $^{+}$significantly less than light (+) WT animals. KO, knockout.

Calcium-binding proteins maintain the Ca^{2+} homeostasis needed for normal cellular function and prevention of neural degeneration (Heizmann, 1993). Retinal projections to the SCN use the excitatory transmitter, glutamate, to communicate light information (Morin & Allen, 2005), and core SCN cells may contain CalB early postnatally to protect against prolonged cellular stimulation by buffering calcium.

In some CalB−/− animals, sparing of a small number of core cells may allow for weak coupling of shell oscillators manifested as low-amplitude free-running rhythms. This finding would be consistent with results in hamster, where a small number of core cells are sufficient to maintain circadian rhythmicity (Kriegsfeld *et al.*, 2004).

Although not examined in the present series of studies, CalB expression is seen in the intergeniculate leaflet (IGL; (Costa & Britto, 1997; Silver *et al.*, 1999; Grubb & Thompson, 2004). The retina projects to the IGL, which in turn projects to the SCN, providing an indirect entrainment pathway (Morin & Allen, 2005). Additionally, the IGL has been implicated in entrainment to a skeleton photoperiod (Edelstein & Amir, 1999). Whether or not the loss of CalB in the IGL accounts for alterations in entrainment or circadian function remains to be examined.

Mice lacking the VPAC2 receptor (Vipr2−/−) receptor exhibit circadian abnormalities similar in some aspects to those seen in CalB−/− mice (Cutler *et al.*, 2003; Hughes *et al.*, 2004). Like CalB−/− mice, a subset of Vipr2−/− animals become arrhythmic in constant conditions and exhibit abnormal entrainment. The mechanisms underlying the rescue of rhythmic behavior in a subset of Vipr2−/− and CalB−/− mice require further study. Unlike CalB−/− mice, however, mice lacking the VPAC2 receptor exhibit abnormal responses to acute light pulses (Hughes *et al.*, 2004). At the cellular level, molecular rhythms in individual SCN cells and the synchronization among SCN neurons are disrupted in mice lacking Vipr2 (Brown *et al.*, 2005; Maywood *et al.*, 2006). These disruptions are abated following GRP treatment (Brown *et al.*, 2005; Maywood *et al.*, 2006). Whether or not loss of synchrony among SCN oscillators accounts for the blunted rhythms of clock gene expression in CalB−/− is not known. Because VIP (endogenous ligand for the VPAC2 receptor) and GRP are co-expressed in a subset of SCN cells (Kawamoto *et al.*, 2003), redundancy in neurochemical secretion may allow GRP to compensate for the actions of VIP. During development, CalB expression overlaps that of VIP- and GRP-immunoreactive cell body labeling, and disruption of CalB may lead to abnormal cell signaling and a behavioral phenotype similar to that of Vipr2−/− animals.

In addition to alterations in SCN function, deficits in entrainment in CalB−/− animals may also result from abnormal retinal signaling to the circadian system. We found that CalB is co-expressed in retinal melanopsin-expressing ganglion cells in adult WT mice (Fig. 5), suggesting a role in the circadian visual system. These cells project to the SCN and are crucial for regulating photic entrainment (Berson *et al.*, 2002; Hannibal & Fahrenkrug, 2002; Panda *et al.*, 2002b; Hattar *et al.*, 2003). In addition to being directly photoresponsive, melanopsin-expressing ganglion cells also receive inputs from retinal circuits activated by conventional rod and cone photoreceptors, thus making them responsive to light inputs through two distinct mechanisms. The light-induced responses of melanopsin-containing ganglion cells mediated by rod and cone inputs are relatively transient (Perez-Leon *et al.*, 2006), whereas those generated through melanopsin can be sustained (Berson *et al.*, 2002; Tu *et al.*, 2005). Light-induced activation of melanopsin releases calcium from internal stores (Kumbalasiri *et al.*, 2007), suggesting the possibility that a rise in internal calcium levels may underlie a cascade that contributes to the longevity of the light-induced response. The loss of CalB in adulthood, and perhaps earlier in development, might interfere with this putative cascade, and this reduction in a sustained retinal response may underlie deficits associated with effects of tonic light exposure on circadian period in CalB−/− mice, a possibility that remains an interesting topic for future investigation.

The present series of studies has revealed a novel role for CalB in mouse circadian rhythm generation and entrainment. These results point to a role for CalB in retina and SCN during adulthood and development, respectively. Additionally, the present findings suggest that the ability to phase shift is not equivalent to entrainment, as CalB−/− mice respond normally to acute light presentation but fail to entrain normally to a LD cycle. These findings set the stage for further exploration of the mechanistic basis of circadian rhythm maintenance and the transmission and reception of photic stimuli.

Acknowledgements

This work was supported by the National Institutes of Health Grant NS37919 (R.S.) and the Richard H. Chartrand Foundation (P.W.), and the University of California Committee on Research Grants (L.J.K.). We thank Dr I. Provencio and David Berson for a generous gift of anti-melanopsin antibody and its antigenic peptide.

Abbreviations

CalB, calbindin $D_{28K;}$ CT, circadian time; DAB, diaminobenzidine; DD, constant darkness; GRP, gastrin-releasing peptide; KO, knockout; LD, light : dark; OD, optical density; P, postnatal day; PB, phosphate buffer; PBS, phosphate-buffered saline; PCR, polymerase chain reaction; SCN, suprachiasmatic nucleus; VIP, vasoactive intestinal peptide;WT, wild-type; ZT, zeitgeber time.

References

Airaksinen, M.S., Eilers, J., Garaschuk, O., Thoenen, H., Konnerth, A. & Meyer, M. (1997) Ataxia and altered dendritic calcium signaling in mice carrying a targeted null mutation of the calbindin D28k gene. *Proc. Natl Acad. Sci. U. S. A.*, **94**, 1488–1493.

Antle, M.C. & Silver, R. (2005) Orchestrating time: arrangements of the brain circadian clock. *Trends Neurosci.*, **28**, 145–151.

Antle, M.C., Foley, D.K., Foley, N.C. & Silver, R. (2003) Gates and oscillators: a network model of the brain clock. *J. Biol. Rhythms*, **18**, 339–350.

Antle, M.C., Foley, N.C., Foley, D.K. & Silver, R. (2007) Gates and oscillators II: Zeitgebers and the network model of the brain clock. *J. Biol. Rhythms*, **22**, 14–25.

Bennis, M., Versaux-Botteri, C., Reperant, J. & Armengol, J.A. (2005) Calbindin, calretinin and parvalbumin immunoreactivity in the retina of the chameleon (*Chamaeleo chamaeleon*). *Brain Behav. Evol.*, **65**, 177–187.

Berson, D.M., Dunn, F.A. & Takao, M. (2002) Phototransduction by retinal ganglion cells that set the circadian clock. *Science (New York, N.Y.)*, **295**, 1070–1073.

Brown, T.M., Hughes, A.T. & Piggins, H.D. (2005) Gastrin-releasing peptide promotes suprachiasmatic nuclei cellular rhythmicity in the absence of vasoactive intestinal polypeptide-VPAC2 receptor signaling. *J. Neurosci.*, **25**, 11155–11164.

Bryant, D.N., LeSauter, J., Silver, R. & Romero, M.T. (2000) Retinal innervation of calbindin-D28K cells in the hamster suprachiasmatic nucleus: ultrastructural characterization. *J. Biol. Rhythms*, **15**, 103–111.

Chiquet, C., Dkhissi-Benyahya, O. & Cooper, H.M. (2005) Calcium-binding protein distribution in the retina of strepsirhine and haplorhine primates. *Brain Res. Bull.*, **68**, 185–194.

Costa, M.S. & Britto, L.R. (1997) Calbindin immunoreactivity delineates the circadian visual centers of the brain of the common marmoset (*Callithrix jacchus*). *Brain Res. Bull.*, **43**, 369–373.

Cutler, D.J., Haraura, M., Reed, H.E., Shen, S., Sheward, W.J., Morrison, C.F., Marston, H.M., Harmar, A.J. & Piggins, H.D. (2003) The mouse VPAC2 receptor confers suprachiasmatic nuclei cellular rhythmicity and responsiveness to vasoactive intestinal polypeptide in vitro. *Eur. J. Neurosci.*, **17**, 197–204.

Edelstein, K. & Amir, S. (1999) The role of the intergeniculate leaflet in entrainment of circadian rhythms to a skeleton photoperiod. *J. Neurosci.*, **19**, 372–380.

Foster, R.G., Provencio, I., Hudson, D., Fiske, S., De Grip, W. & Menaker, M. (1991) Circadian photoreception in the retinally degenerate mouse (rd/rd). *J. Comp. Physiol.*, **169**, 39–50.

Grubb, M.S. & Thompson, I.D. (2004) Biochemical and anatomical subdivision of the dorsal lateral geniculate nucleus in normal mice and in mice lacking the beta2 subunit of the nicotinic acetylcholine receptor. *Vision Res.*, **44**, 3365–3376.

Hamada, T., LeSauter, J., Venuti, J.M. & Silver, R. (2001) Expression of period genes: rhythmic and nonrhythmic compartments of the suprachiasmatic nucleus pacemaker. *J. Neurosci.*, **21**, 7742–7750.

Hamada, T., LeSauter, J., Lokshin, M., Romero, M.T., Yan, L., Venuti, J.M. & Silver, R. (2003) Calbindin influences response to photic input in suprachiasmatic nucleus. *J. Neurosci.*, **23**, 8820–8826.

Hannibal, J. & Fahrenkrug, J. (2002) Melanopsin: a novel photopigment involved in the photoentrainment of the brain's biological clock? *Ann. Med.*, **34**, 401–407.

Hattar, S., Liao, H.W., Takao, M., Berson, D.M. & Yau, K.W. (2002) Melanopsin-containing retinal ganglion cells: architecture, projections, and intrinsic photosensitivity. *Science (New York, N.Y.)*, **295**, 1065–1070.

Hattar, S., Lucas, R.J., Mrosovsky, N., Thompson, S., Douglas, R.H., Hankins, M.W., Lem, J., Biel, M., Hofmann, F., Foster, R.G. & Yau, K.W. (2003) Melanopsin and rod-cone photoreceptive systems account for all major accessory visual functions in mice. *Nature*, **424**, 76–81.

Heizmann, C.W. (1993) Calcium signaling in the brain. *Acta Neurobiol. Exp. (Wars)*, **53**, 15–23.

Hughes, A.T., Fahey, B., Cutler, D.J., Coogan, A.N. & Piggins, H.D. (2004) Aberrant gating of photic input to the suprachiasmatic circadian pacemaker of mice lacking the VPAC2 receptor. *J. Neurosci.*, **24**, 3522–3526.

Jin, X., Shearman, L.P., Weaver, D.R., Zylka, M.J., de Vries, G.J. & Reppert, S.M. (1999) A molecular mechanism regulating rhythmic output from the suprachiasmatic circadian clock. *Cell*, **96**, 57–68.

Jobst, E.E. & Allen, C.N. (2002) Calbindin neurons in the hamster suprachiasmatic nucleus do not exhibit a circadian variation in spontaneous firing rate. *Eur. J. Neurosci.*, **16**, 2469–2474.

Karatsoreos, I., Yan, L., LeSauter, J. & Silver, R. (2004a) Rhythmic and nonrhythmic compartments of Per1 expression in mouse SCN. *J. Neurosci.*, **24**, 68–75.

Karatsoreos, I.N., Yan, L., LeSauter, J. & Silver, R. (2004b) Phenotype matters: identification of light-responsive cells in the mouse suprachiasmatic nucleus. *J. Neurosci.*, **24**, 68–75.

Kawamoto, K., Nagano, M., Kanda, F., Chihara, K., Shigeyoshi, Y. & Okamura, H. (2003) Two types of VIP neuronal components in rat suprachiasmatic nucleus. *J. Neurosci. Res.*, **74**, 852–857.

Kriegsfeld, L.J., LeSauter, J. & Silver, R. (2004) Targeted microlesions reveal novel organization of the hamster suprachiasmatic nucleus. *J. Neurosci.*, **24**, 2449–2457.

Kriegsfeld, L.J., Mei, D.F., Bentley, G.E., Ubuka, T., Mason, A.O., Inoue, K., Ukena, K., Tsutsui, K. & Silver, R. (2006) Identification and characterization of a gonadotropin-inhibitory system in the brains of mammals. *Proc. Natl Acad. Sci. U. S. A.*, **103**, 2410–2415.

Kumbalasiri, T., Rollag, M.D., Isoldi, M., de Lauro Castrucci, A.M. & Provencio, I. (2007) Melanopsin triggers the release of internal calcium stores in response to light. *Photochem. Photobiol.*, **83**, 273–279.

LeSauter, J. & Silver, R. (1999) Localization of a suprachiasmatic nucleus subregion regulating locomotor rhythmicity. *J. Neurosci.*, **19**, 5574–5585.

LeSauter, J., Yan, L., Vishnubhotla, B., Quintero, J.E., Kuhlman, S.J., McMahon, D.G. & Silver, R. (2003) A short half-life GFP mouse model for analysis of suprachiasmatic nucleus organization. *Brain Res.*, **964**, 279–287.

Maywood, E.S., Reddy, A.B., Wong, G.K., O'Neill, J.S., O'Brien, J.A., McMahon, D.G., Harmar, A.J., Okamura, H. & Hastings, M.H. (2006) Synchronization and maintenance of timekeeping in suprachiasmatic circadian clock cells by neuropeptidergic signaling. *Curr. Biol.*, **16**, 599–605.

Moore, R.Y. (1996) Entrainment pathways and the functional organization of the circadian system. *Prog. Brain Res.*, **111**, 103–119.

Moore, R.Y. & Eichler, V.B. (1972) Loss of a circadian adrenal corticosterone rhythm following suprachiasmatic lesions in the rat. *Brain Res.*, **42**, 201–206.

Morin, L.P. & Allen, C.N. (2005) The circadian visual system. *Brain Res. Rev.*, **51**, 1–60.

Mrosovsky, N. (1999) Masking: history, definitions, and measurement. *Chronobiol. Int.*, **16**, 415–429.

Nelson, D.E. & Takahashi, J.S. (1991a) Comparison of visual sensitivity for suppression of pineal melatonin and circadian phase-shifting in the golden hamster. *Brain Res.*, **554**, 272–277.

Nelson, D.E. & Takahashi, J.S. (1991b) Sensitivity and integration in a visual pathway for circadian entrainment in the hamster (*Mesocricetus auratus*). *J. Physiol.*, **439**, 115–145.

Okamura, H., Yamaguchi, S. & Yagita, K. (2002) Molecular machinery of the circadian clock in mammals. *Cell Tissue Res.*, **309**, 47–56.

Panda, S., Hogenesch, J.B. & Kay, S.A. (2002a) Circadian rhythms from flies to human. *Nature*, **417**, 329–335.

Panda, S., Sato, T.K., Castrucci, A.M., Rollag, M.D., DeGrip, W.J., Hogenesch, J.B., Provencio, I. & Kay, S.A. (2002b) Melanopsin (Opn4) requirement for normal light-induced circadian phase shifting. *Science (New York, N.Y.)*, **298**, 2213–2216.

Perez-Leon, J.A., Warren, E.J., Allen, C.N., Robinson, D.W. & Lane Brown, R. (2006) Synaptic inputs to retinal ganglion cells that set the circadian clock. *Eur. J. Neurosci.*, **24**, 1117–1123.

Provencio, I., Rodriguez, I.R., Jiang, G., Hayes, W.P., Moreira, E.F. & Rollag, M.D. (2000) A novel human opsin in the inner retina. *J. Neurosci.*, **20**, 600–605.

Schibler, U. (2005) The daily rhythms of genes, cells and organs. Biological clocks and circadian timing in cells. *EMBO Rep*, **6** Spec No, S9–S13.

Silver, R., Sookhoo, A.I., LeSauter, J., Stevens, P., Jansen, H.T. & Lehman, M.N. (1999) Multiple regulatory elements result in regional specificity in circadian rhythms of neuropeptide expression in mouse SCN. *Neuroreport*, **10**, 3165–3174.

Stephan, F.K. & Zucker, I. (1972) Rat drinking rhythms: central visual pathways and endocrine factors mediating responsiveness to environmental illumination. *Physiol. Behav.*, **8**, 315–326.

Tu, D.C., Zhang, D., Demas, J., Slutsky, E.B., Provencio, I., Holy, T.E. & Van Gelder, R.N. (2005) Physiologic diversity and development of intrinsically photosensitive retinal ganglion cells. *Neuron*, **48**, 987–999.

Van der Veen, D.R., Castillo, M.R., Van der Zee, E.A., Jansen, K., Gerkema, M.P. & Bult-Ito, A. (2005) Circadian dynamics of vasopressin in mouse selection lines: translation and release in the SCN. *Brain Res.*, **1060**, 16–25.

Wassle, H., Peichl, L., Airaksinen, M.S. & Meyer, M. (1998) Calcium-binding proteins in the retina of a calbindin-null mutant mouse. *Cell Tissue Res.*, **292**, 211–218.

Wee, R., Castrucci, A.M., Provencio, I., Gan, L. & Van Gelder, R.N. (2002) Loss of photic entrainment and altered free-running circadian rhythms in math5-/- mice. *J. Neurosci.*, **22**, 10427–10433.

Yan, L. & Okamura, H. (2002) Gradients in the circadian expression of Per1 and Per2 genes in the rat suprachiasmatic nucleus. *Eur. J. Neurosci.*, **15**, 1153–1162.

Yan, L. & Silver, R. (2004) Resetting the brain clock: time course and localization of mPER1 and mPER2 protein expression in suprachiasmatic nuclei during phase shifts. *Eur. J. Neurosci.*, **19**, 1105–1109.